Influences of ZnO sol-gel thin film characteristics on ZnO nanowire arrays prepared at low temperature using all solution-based processing

Jing-Shun Huang
Institute of Photonics and Optoelectronics, National Taiwan University, Taipei, 10617 Taiwan, Republic of China

Ching-Fuh Lin[a)]
Institute of Photonics and Optoelectronics, Graduate Institute of Electronics Engineering, National Taiwan University, Taipei, 10617 Taiwan, Republic of China and Department of Electrical Engineering, National Taiwan University, Taipei, 10617 Taiwan, Republic of China

(Received 10 September 2007; accepted 2 November 2007; published online 3 January 2008)

Zinc oxide (ZnO) nanowire arrays with controlled nanowire diameter, crystal orientation, and optical property were prepared on sol-gel ZnO-seed-coated substrates with different pretreatment conditions by a hydrothermal method. The vertical alignment, crystallinity, and defect density of ZnO nanowire arrays are found to be strongly dependent on the characteristics of the ZnO thin films. Field-emission scanning electron microscopy, energy dispersive spectroscopy, x-ray diffraction, and room temperature photoluminescence were applied to analyze the quality of the ZnO nanowire arrays. The annealing temperature of the ZnO thin film plays an important role on the microstructure of the ZnO grains and then the growth of the ZnO nanowire arrays. The x-ray diffraction results indicate that the thin film annealed at the low temperature of 130 °C is amorphous, but the thereon nanowire arrays are high-quality single crystals growing along the *c*-axis direction with a high consistent orientation perpendicular to the substrates. The as-synthesized ZnO nanowire arrays via all solution-based processing enable the fabrication of next-generation nanodevices at low temperature. © *2008 American Institute of Physics*. [DOI: 10.1063/1.2828172]

I. INTRODUCTION

One-dimensional (1D) nanowires have been extensively studied in recent years. Among these materials, zinc oxide (ZnO) nanowires have attracted great interest for promising applications in optoelectronics devices such as room temperature lasers,[1] light emitting diodes,[2–5] ultraviolet (UV) detectors,[6] field-emission displays,[7–9] photonic crystals,[10] and solar cells.[11–14] ZnO is a wide band gap (3.37 eV) semiconductor with a large exciton binding energy (60 meV), exhibiting near-UV light emission, transparent conductivity, and piezoelectricity.[15] Several methods have been demonstrated to fabricate 1D ZnO nanostructures, such as vapor-liquid-solid epitaxy (VLSE), chemical vapor deposition (CVD), and pulse laser deposition (PLD), but these gas phase techniques still have some limitations for substrate size and the need for high temperature operation [above 800 °C for VLSE (Ref. 16) and 500 °C for CVD method[17]]. Recently, the growth of ZnO nanowires and microrods in aqueous solutions at low temperature was reported by using the hydrothermal process.[18] Hydrothermal process has shown the possibility for applications in light emitting diodes and solar cells with their growth temperature below 100 °C and easy scale up. This aqueous-based technique has also been used successfully to demonstrate the fabrication of large arrays of vertical ZnO nanowires on glass, 4 in. diameter Si wafers,[19] and plastic substrates.[7] This stimulated the study of using ZnO nanowire arrays on plastic substrates for application in flexible electronic devices.

However, these device applications might be reinforced if the position, orientation, and shape of nanostructures can be controlled to a high degree of precision. The selective growth of ZnO nanostructures on desired areas of Si substrates by using lithography process has been reported.[7,10,20]. Bekeny *et al.*[21] reported that the size of ZnO nanowires varied with the molar composition of the chemical precursors. Li *et al.*[22] reported that the growth of different morphologies of ZnO nanowires was dependent on substrate temperature in the PLD process. Guo *et al.*[23] reported that the diameter and length of ZnO nanowire arrays were controlled at different growth temperatures under hydrothermal conditions. Although Ma *et al.*[24] reported that an annealing treatment of the substrate can influence the density of the ZnO nanowire arrays on indium tin oxide (ITO), there is no study on crystallinity and photoluminescence of ZnO nanowire arrays. Moreover, Kang *et al.*[25] reported that the shape of the ZnO nanowires was sensitive to the orientation of Si substrate via the use of ZnO nanoparticles as a seed layer. However, systematic research on the influence of quality characteristics of ZnO sol-gel thin films on the growth of ZnO nanowire arrays via hydrothermal method has rarely been reported.

In this work, we systematically study the feature-controlled ZnO nanowire arrays via the hydrothermal method and ZnO sol-gel thin films were used as the seed layers with different pretreatment conditions. Our investigation shows that the vertical alignment, the crystallinity, and

[a)]Author to whom correspondence should be addressed. Tel: 886-2-3366 3540. FAX: 886-2-2364 2603. Electronic mail: cflin@cc.ee.ntu.edu.tw.

the defect density of ZnO nanowire arrays are strongly dependent on the characteristics of the thin films. Field-emission scanning electron microscopy (FESEM), energy dispersive spectroscopy (EDS), x-ray diffraction (XRD) pattern, and room temperature photoluminescence (PL) spectrum were applied to analyze the quality of so produced ZnO nanowire arrays.

II. EXPERIMENTAL DETAILS

The ZnO thin films served as the seed layers were deposited on silicon substrates by a sol-gel method.[26] A coating solution contained zinc acetate dihydrate [$Zn(CH_3COO)_2 2H_2O$, Merck, 99.5% purity] and equivalent molar monoethanolamine (MEA) ($NH_2CH_2CH_2OH$, Merck, 99.5% purity) dissolved in 2-methoxyethanol (2MOE) ($CH_3OCH_2CH_2OH$, Merck, 99.5% purity). The concentration of zinc acetate was chosen to be 0.5 mol. The resulting solution was then stirred at 60 °C for 2 h to yield a homogeneous and stable colloid solution, which served as the coating solution after being cooled to room temperature. Then the solution was coated onto *p*-type silicon (100) substrates by a spin coater at the rate of 1000 rpm for 20 s and then 3000 rpm for 30 s at room temperature. Subsequently, the gel films were preheated for 10 min to remove the residual solvent. The procedures from coating to preheating were repeated ten times. Then the ten-layer films were annealed in a furnace at different temperatures ranging from 130 to 900 °C for 1 h.

After uniformly coating the silicon substrates with ZnO thin films, hydrothermal growth of ZnO nanowire arrays was achieved by suspending these ZnO seed-coated substrates upside down in a glass beaker filled with aqueous solution of 50 mM zinc nitrate hexahydrate [$Zn(NO_3)_2 6H_2O$, Sigma Aldrich, 98% purity] and 50 mM hexamethylenetetramine (HMT) ($C_6H_{12}N_4$, Sigma Aldrich, 99.5% purity). During the growth, the glass beaker was heated with a laboratory oven and maintained at 90 °C for 4 h. At the end of the growth period, the substrates were removed from the solution, then immediately rinsed with de-ionized water to remove any residual salt from the surface, and dried in air at room temperature. The general morphologies of the ZnO thin films and thereon ZnO nanowire arrays were examined by FESEM. An EDS spectrum of the ZnO nanowires was measured with the same SEM system. The crystal phase and crystallinity were analyzed at room temperature by XRD using Cu $K\alpha$ radiation. The room temperature PL, measured using a Nd:yttrium aluminum garnet (YAG) laser at 266 nm as the exciting source, was used to characterize the optical properties of the ZnO thin films and thereon ZnO nanowire arrays.

III. RESULTS AND DISCUSSION

Figure 1 shows the top view FESEM images for the surface morphologies of ZnO sol-gel thin films and thereon ZnO nanowire arrays at different annealing temperatures of the thin films. Figures 1(a), 1(c), 1(e), and 1(g) indicate that the grains of thin films reveal a noticeable transformation with increasing annealing temperatures from 130 to 900 °C. At the annealing temperature of 130 °C, no grain forms and the surface is smooth. At the annealing temperature of 300 °C, the film contains fine grains and the particle size is about 80 nm. Once the annealing temperature increases, the grains become larger and densely packed. This result concerned with the annealing temperature is consistent with the result of the research of Wang *et al.*[27] It demonstrates that the quality of ZnO thin film was improved due to the redistribution of crystalline grain by supplying sufficient thermal energy and the small grain has been joined into great crystalline surface.

Figures 1(b), 1(d), 1(f), and 1(h) show the ZnO nanowire arrays corresponding to Figs. 1(a), 1(c), 1(e), and 1(g), respectively. They were grown at a fixed temperature (90 °C), while the thin films were annealed at 130, 300, 600, and 900 °C, respectively. They show that the obtained ZnO nanowire arrays are typically hexagonal-shaped. As the annealing temperatures of the ZnO thin films increase from 130 to 900 °C, the diameters of the ZnO nanowire arrays increase from 60 to 260 nm. The reason may be that the high annealing temperature evidently enhances the interaction among the grains and leads the grains to merge together to form bigger ZnO seeds, and thus increases the diameter of the ZnO nanowires thereon. Therefore, the size of the grains is a key factor that influences the nucleation of ZnO nanowire arrays. Furthermore, it is notable that the ZnO nanowire arrays on the ZnO thin films annealed at 130 °C are well-aligned vertically and uniformly [Fig. 1(b)], and the well-defined crystallographic planes of the hexagonal single-crystalline nanowires can be clearly identified, providing a strong evidence that the nanowire arrays orientate along the *c*-axis.

Figure 2(a) gives the XRD patterns of those ZnO thin films annealed at 130, 300, 600 and 900 °C, respectively. The XRD patterns reveal that the (002) peak intensity varies with annealing temperature. When the ZnO thin films are annealed below 300 °C, there is no preferred (002) *c*-axis orientation. At the temperature of 600 °C, (100), (002), (101), (102), and (110) diffraction peaks corresponding to the ZnO wurtzite structure are observed in the XRD pattern, where the preferred (002) *c*-axis orientation dominates. This reason may be that the use of 2MOE and MEA solvents of higher boiling points has resulted in a strongly preferred (002) orientation.[28] When the annealing temperature increases to 900 °C, the polycrystalline structure emerges with the (100) and (101) peaks while the intensity of the (002) peak decreases. This result indicates that the crystalline quality of each grain becomes poor.[29] Therefore, we may conclude that the preferred *c*-axis orientation initially increases with annealing temperature until it reaches the optimal situation at a certain annealing temperature. Afterwards the *c*-axis orientation intensity decreases gradually.

Figure 2(b) shows the XRD patterns of the ZnO nanowire arrays corresponding to those shown in Fig. 2(a). Please note again that the nanowire arrays are grown at the same temperature of 90 °C, while the thin films were annealed from 130 to 900 °C. The peaks in the x-ray diffraction patterns are indexed to the hexagonal phase of ZnO. It is found that no other characteristic peaks corresponding to the impu-

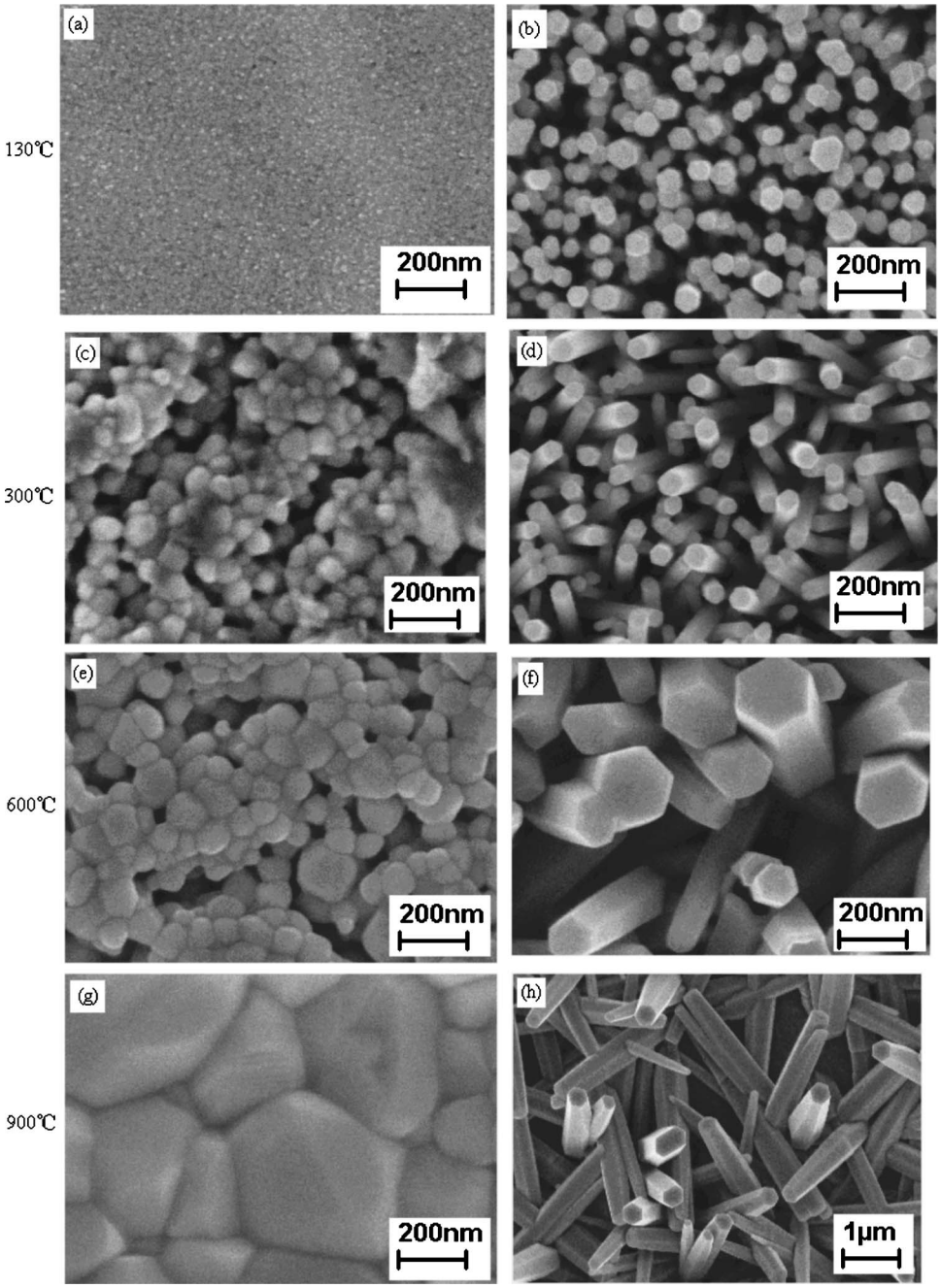

FIG. 1. FESEM images of ZnO sol-gel thin films with annealing at (a) 130 °C, (c) 300 °C, (e) 600 °C, and (g) 900 °C. (b), (d), (f), and (h) show the ZnO nanowire arrays were grown at a fixed temperature (90 °C), while the thin films were annealed at 130, 300, 600, and 900 °C, respectively. The grain sizes become larger and denser with increasing annealing temperature, which results in the increasing of the diameter of ZnO nanowire arrays.

rities of the precursors such as zinc nitrate and zinc hydroxide are observed in the XRD patterns. At the temperatures of 130, 300, and 600 °C, only a very strong (002) diffraction peak and a very weak (101) peak are observed, indicating that the three ZnO samples are all of high *c*-axis orientation. It is noticeable that for the sample annealed at 130 °C the XRD pattern shows only the (002) diffraction peak. In addition, the intensity of (002) diffraction peak is strongest, compared to other samples annealed at higher temperatures. This implies its perfect *c*-axis orientation and this result is in accordance with its SEM image [Fig. 1(b)]. On the other hand, for the sample annealed at 900 °C, the (002) diffraction peak becomes weak, and at the same time, the (100) and (101) peaks become strong, indicating its tendency toward random orientation. It means that the films annealed at 900 °C has worse morphology [Fig. 1(g)] and hence results in the relatively random orientation of nanowire arrays as observed in the Fig. 1(h).

It is interesting to note that the (002) diffraction peak of the seed layer annealed at 130 °C is smaller than that at 600 °C, while the (002) diffraction peak of thereon ZnO nanowire arrays at 130 °C is larger than that at 600 °C. The previous investigation of the thin films annealed at 130 °C indicates that it is nearly amorphous. However, the growth of ZnO nanowire arrays on amorphous ZnO thin films along the (002) plane is even more notable than that on polycrystalline thin films. It may be because the polycrystalline ZnO grains with a certain orientation limit the growth along the (002) plane. In comparison, the amorphous ZnO seed layer does not limit the growth along the (002) plane. This indicates that the ZnO nanowire arrays prepared by the hydrothermal

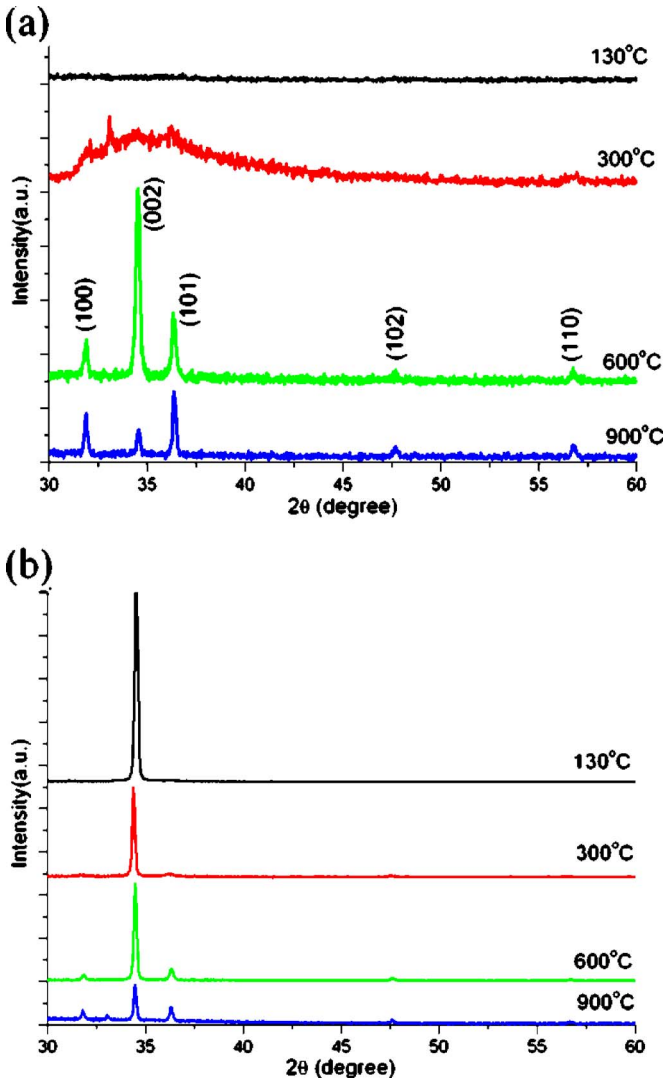

FIG. 2. (Color online) XRD spectra of (a) ZnO seed layers annealed from 130 to 900 °C and (b) thereon ZnO nanowire arrays.

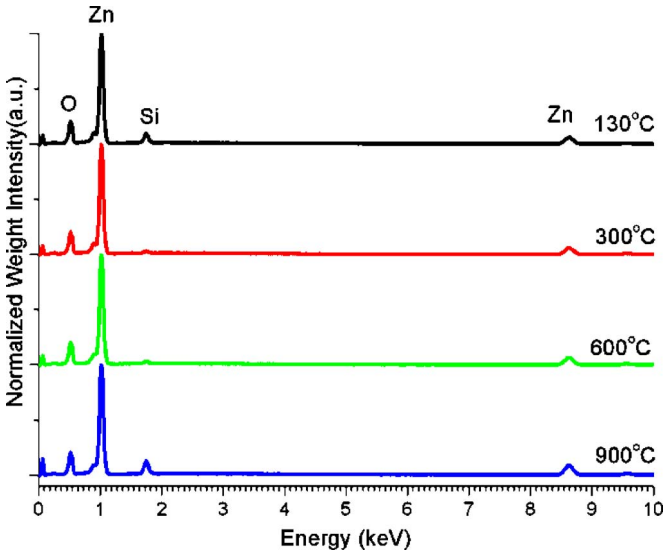

FIG. 3. (Color online) EDS spectra of ZnO nanowire arrays with ZnO seed layers annealed from 130 to 900 °C.

method have preferential orientation along the (002) plane, in particular, on the thin films without a certain orientation.

Figure 3 shows the chemical composition of the ZnO nanowire arrays determined by the typical EDS. The peak at 0.5 keV is from oxygen and peaks at 0.9 and 8.6 keV are due to Zn. The peak at 1.7 keV is from the silicon substrates. Besides silicon, the EDS spectra reveal the presence of Zn and O elements, which confirms that the nanowire arrays are primarily ZnO.

Figure 4(a) shows the room temperature PL spectra of a set of ZnO thin films annealed at different temperatures. From this figure, an evident ultraviolet near-band edge emission peak at 385 nm is observed, which originates from the excitonic recombination. As the annealing temperature increases from 130 to 900 °C, the PL peak in the UV region is gradually enhanced. It is believed that the higher annealing temperatures facilitate the migration of grain boundaries and promote the coalescence of small crystals, and thus reduce the concentration of nonradiative recombination centers. However, at the temperature of 900 °C, defects related to deep-level emission around 500–550 nm from the ZnO nanowire arrays were also observed. This defect-related green emission is believed to come from oxygen vacancies. At the temperatures of 130 °C, the ZnO thin films may not form a good crystal phase, and hence the UV emission intensity is very low. Therefore, we may conclude that as the thin-film annealing temperature increases the UV peak increases but the peak in the green region also increases, indicating that the oxygen vacancies abruptly increase at high temperature due to the volatilization of Zn atom.

The room temperature PL characteristics of thereon ZnO nanowire arrays with different annealing temperatures of thin films are shown in Fig. 4(b). The UV peak increases with annealing temperature. The UV emission of ZnO nanowire arrays corresponding to the near-band edge emission is due to the recombination of free excitons through an exciton-exciton collision process.

At the temperature of 900 °C, the defect-related green emission of the nanowire arrays is lower than that of the seed layers. The green emission is also known to be a deep level emission caused by the impurities and structural defects in the crystal such as oxygen vacancies, zinc interstitials, and so on.[30] Therefore, it is suggested that the nanowire arrays may reduce the defect density and hence lower the defect-related emission caused by the thin films.

At low temperatures of 130 and 300 °C, the ZnO nanowire arrays exhibits a larger UV emission than ZnO thin films, indicating that the nanowire arrays do enhance the UV emission. Moreover, at the temperature of 130 °C, the ZnO nanowire arrays have a highly preferred (002) orientation and vertical alignment.

IV. CONCLUSION

In summary, our work provides a systematic study of feature-controlled ZnO nanowire arrays via the hydrothermal method. Our investigation demonstrates that the sol-gel thin-film pretreatment conditions have strong influences on the features of the ZnO nanowire arrays grown thereon. The annealing temperature of the ZnO sol-gel thin film can affect the microstructure of the ZnO grains and then the growth of

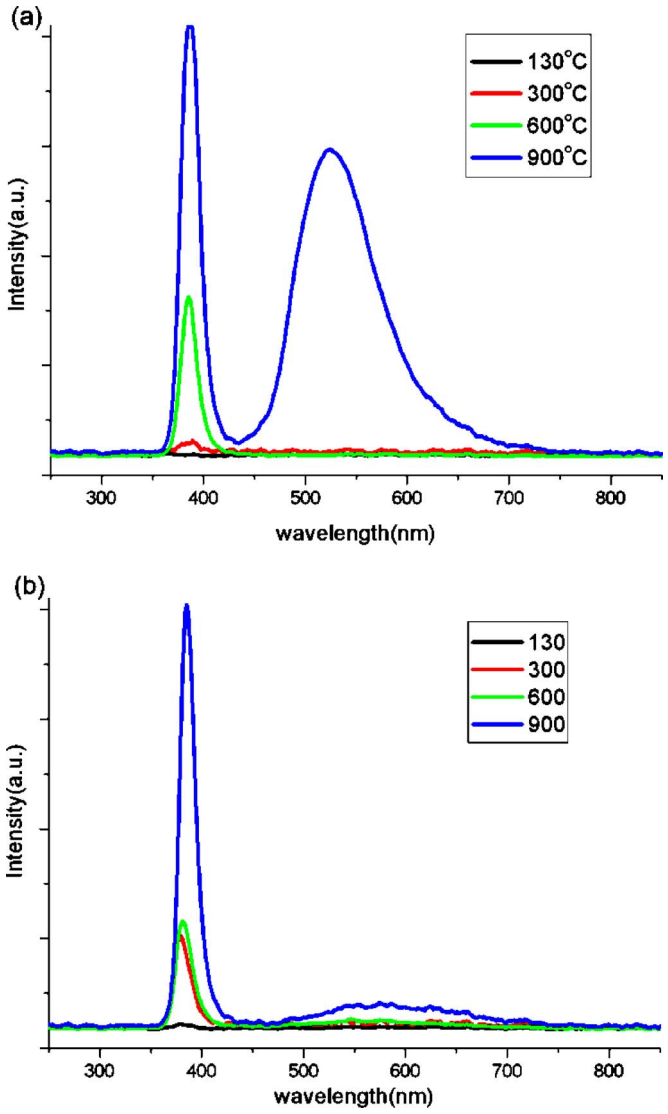

FIG. 4. (Color online) Room temperature PL spectra of (a) ZnO seed layers and (b) thereon ZnO nanowire arrays with annealing temperature of ZnO seed layers from 130 to 900 °C for 1 h in air (excitation wavelength: 266 nm)

the ZnO nanowire arrays. As the annealing temperature increases from 130 to 900 °C, the grain size of the thin films increases, and the diameter of thereon ZnO nanowire arrays increases from 60 to 260 nm. The *c*-axis orientation of the thin films also increases with the annealing temperature until it reaches the optimal situation at a certain annealing temperature and then gradually decreases. However, the (002) diffraction peak of thereon ZnO nanowire arrays decreases with annealing temperature. The thin films influence the nucleation of the ZnO and subsequently affect the diameter and orientation of the thereon nanowire arrays. At the temperature of 130 °C, the ZnO nanowire arrays align very vertically with growth along the *c*-axis direction. The PL measurements show a strong and dominant UV emission at 385 nm, indicating that the low-temperature growth results in low levels of oxygen vacancies in the nanowires. This work provides all solution-based processing route to fabrication of low-cost highly oriented ZnO nanowire arrays at low temperature. These vertical nanowire arrays are highly suitable for use in ordered nanowire-polymer devices, such as solar cells and light emitting diodes.

ACKNOWLEDGMENTS

This work was supported by the National Science Council, Taiwan, Republic of China, with Grant Nos. NSC96-2221-E-002-277-MY3 and NSC96-2218-E-002-025.

[1]M. H. Huang, S. Mao, H. Feick, H. Yan, Y. Wu, H. Kind, E. Weber, R. Russo, and P. Yang, Science **292**, 1897 (2001).
[2]J. Nause, M. Pan, V. Rengarajan, W. Nemeth, S. Ganesan, A. Payne, N. Li, and I. Ferguson, Proc. SPIE **5941**, 70 (2005).
[3]Y. Ryu, T. S. Lee, J. A. Lubguban, H. W. White, B. J. Kim, Y. S. Park, and C. J. Youn, Appl. Phys. Lett. **88**, 241108 (2006).
[4]S. H. Park, S. H. Kim, and S. W. Han, Nanotechnology **18**, 055608 (2007).
[5]Z. P. Wei, Y. M. Lu, D. Z. Shen, Z. Z. Zhang, B. Yao, B. H. Li, J. Y. Zhang, D. X. Zhao, X. W. Fan, and Z. K. Tang, Appl. Phys. Lett. **90**, 042113 (2007).
[6]C. Y. Lu, S. J. Chang, S. P. Chang, C. T. Lee, C. F. Kuo, H. M. Chang, Y. Z. Chiou, C. L. Hsu, and I. C. Chen, Appl. Phys. Lett. **89**, 153101 (2006).
[7]J. B. Cui, C. P. Daghlian, U. J. Gibson, R. Pusche, P. Geithner, and L. Ley, J. Appl. Phys. **97**, 044315 (2005).
[8]B. Cao, X. Teng, S. H. Heo, Y. Li, S. O. Cho, G. Li, and W. Cai, J. Phys. Chem. C **111**, 2470 (2007).
[9]W. Wang, G. Zhang, L. Yu, X. Bai, Z. Zhang, and X. Zhao, Physica E (Amsterdam) **36**, 86 (2007).
[10]J. Cui and U. Gibson, Nanotechnology **18**, 155302 (2007).
[11]D. C. Olson, J. Piris, R. T. Collins, S. E. Shaheen, and D. S. Ginley, Thin Solid Films **496**, 26 (2006).
[12]A. M. Peiro, P. Ravirajan, K. Govender, D. S. Boyle, P. O'Brien, D. D. C. Bradley, J. Nelson, and J. R. Durrant, J. Mater. Chem. **16**, 2088 (2006).
[13]P. Ravirajan, A. M. Peiro, M. K. Nazeeruddin, M. Graetzel, D. D. C. Bradley, J. R. Durrant, and J. Nelson, J. Phys. Chem. B **110**, 7635 (2006).
[14]J. Owen, M. S. Son, K. H. Yoo, B. D. Ahn, and S. Y. Lee, Appl. Phys. Lett. **90**, 033512 (2007).
[15]U. Ozgur, Y. I. Alivov, C. Liu, A. Teke, M. A. Reshchikov, S. Dogan, V. Avrutin, S. J. Cho, and H. Morkoc, J. Appl. Phys. **98**, 041301 (2005).
[16]M. H. Huang, Y. Wu, H. Feick, N. Tran, E. Weber, and P. Yang, Adv. Mater. (Weinheim, Ger.) **13**, 113 (2001).
[17]G. Z. Wang, Y. Wang, M. Y. Yau, C. Y. To, C. J. Deng, and D. H. L. Ng, Mater. Lett. **59**, 3870 (2005).
[18]L. Vayssieres, Adv. Mater. (Weinheim, Ger.) **15**, 464 (2003).
[19]L. E. Greene, M. Law, J. Goldberger, F. Kim, J. C. Johnson, Y. F. Zhang, R. J. Saykally, and P. D. Yang, Angew. Chem., Int. Ed. **42**, 3031 (2003).
[20]Y. Tak and K. J. Yong, J. Phys. Chem. B **109**, 19263 (2005).
[21]C. Bekeny, T. Voss, H. Gafsi, J. Gutowski, B. Postels, M. Kreye, and A. Waag, J. Appl. Phys. **100**, 104317 (2006).
[22]C. Li, G. J. Fang, Q. Fu, F. H. Su, G. H. Li, X. G. Wu, and X. Z. Zhao, J. Cryst. Growth **292**, 19 (2006).
[23]M. Guo, P. Diao, X. D. Wang, and S. M. Cai, J. Solid State Chem. **178**, 3210 (2005).
[24]T. Ma, M. Guo, M. Zhang, Y. J. Zhang, and X. D. Wang, Nanotechnology **18**, 035605 (2007).
[25]B. S. Kang, S. J. Pearton, and F. Ren, Appl. Phys. Lett. **90**, 083104 (2007).
[26]M. Ohyama, H. Kouzuka, and T. Yoko, Thin Solid Films **306**, 78 (1997).
[27]M. R. Wang, J. Wang, W. Chen, Y. Cui, and L. D. Wang, Mater. Chem. Phys. **97**, 219 (2006).
[28]M. Rusop, K. Uma, T. Soga, and T. Jimbo, Surf. Rev. Lett. **12**, 697 (2005).
[29]X. Q. Wei, Z. G. Zhang, M. Liu, C. S. Chen, G. Sun, C. S. Xue, H. Z. Zhuang, and B. Y. Man, Mater. Chem. Phys. **101**, 285 (2007).
[30]Q. Ahsanulhaq, A. Umar, and Y. B. Hahn, Nanotechnology **18**, 115603 (2007).